J. Fluid Mech. (1984), *vol.* 142, *pp.* 151–170
Printed in Great Britain

The effect of Langmuir circulation on the distribution of submerged bubbles caused by breaking wind waves

By S. A. THORPE
Institute of Oceanographic Sciences, Wormley, Godalming, Surrey, U.K.

(Received 31 March 1983 and in revised form 13 January 1984)

Clouds of bubbles are generated at the sea surface by breaking wind waves or by heavy rain. Rows of subsurface bubble clouds have been detected by a bottom-mounted side-scan sonar, and are possibly formed by the effects of Langmuir circulation. A simple equation is devised to describe the effects of the turbulent diffusion of bubbles from the free surface, bubble rise and dissolution, and advection by Langmuir circulation. The equation is solved analytically using a series expansion in which advection is supposed small in comparison with diffusion. The solution provides a quantitative measure of the principal effects produced by the circulation, in particular the distortion of the bubble field, and estimates of the advective flux.

A random-walk numerical model, in which changes occurring in individual bubbles are followed, is tested against the analytical model in the range for which the latter is valid. There is good agreement. The numerical model is useful in extending the solutions to more complex cases which include a broad distribution of bubble sizes, and to ranges in which the analytic solution is invalid. The model is used to quantify the effect of the circulation on the acoustic scattering cross-section of the bubble clouds and to explore differences between the conclusions of earlier models and observations by Johnson & Cooke (1979).

In the appendices an estimate is made of the depth to which bubbles can be carried by the vertical velocities observed below wind rows, and this is found to agree reasonably well with the maximum depth to which bubbles are observed to penetrate. Estimates of mean vertical diffusion coefficients based on observations of bubbles are compared with some calculated solely from the advective flux in Langmuir circulation. The latter are, as expected, smaller than those representing the sum of all the contributions to the flux, but are a significant fraction, of the order of 0.2–0.4. A method of deriving the vertical diffusion coefficient from observations of the vertical distribution of the acoustic scattering cross-section of bubbles appears not to be very sensitive to circulation and may provide estimates within about 25 % of the actual values.

1. Introduction

Langmuir's description of lines of floating weed seen whilst crossing the Atlantic in 1927, and the subsequent extensive measurements in Lake George reported in his celebrated 1938 paper on wind rows, provided a sound observational basis to knowledge of what is now known as Langmuir circulation. Later observers have measured other aspects of the circulation, including the downward vertical velocity below wind rows (Harris & Lott 1973; Filatov, Rjanzhin & Zaycev 1981) and the effect

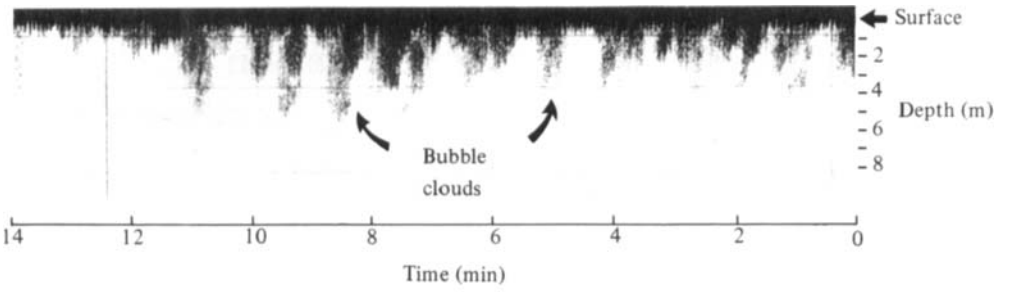

FIGURE 1. A sonograph, depth-versus-time display, of bubble clouds below the surface obtained using a vertically pointing, narrow-beam sonar mounted on the sea bed. The wind speed was about 9 m s^{-1}. (From Thorpe (1982).)

of the circulation on the mean temperature field (McLeish 1968; Scott *et al.* 1969; Thorpe & Hall 1982; see also the review by Pollard 1977). Significant theoretical advances have also been made towards explaining the cause of the circulation. These have been reviewed by Leibovich (1983). A theory in which surface waves play a key role, and which is consistent with the main features of the observed circulation, has been developed by Craik and Leibovich and their collaborators, and some aspects of this have been tested in the laboratory (Faller & Caponi 1978; Faller & Cartwright 1982).

We are not, however, concerned here with the cause of the circulation but rather with its effects. Although Langmuir himself suggested that 'the helical vortices set up by the wind apparently contribute the essential mechanism by which the epilimnion is produced', the importance of the circulation has not been established and it is not known whether, or when (i.e. at what wind speeds) or where (i.e. over what depth range), it dominates over other, perhaps less organized, processes of turbulent diffusion. The accumulation of foam in wind rows is persuasive evidence of its effects on the horizontal diffusion on floating particles at the surface, but subsurface observations are generally less convincing. In particular the existence of braidlike structures in the temperature field of the near-surface mixing region with orientation transverse to the wind direction (Thorpe & Hall 1980) suggests that there are other mechanisms which may be important in promoting vertical diffusion.

Recent sonar observations of subsurface bubbles caused by wind waves breaking in deep water (Thorpe 1982; hereinafter referred to as I) provide a novel technique for examining vertical diffusion in the near-surface zone. Figure 1 is a sonograph record obtained using the bottom-mounted, upward-pointing, narrow-beam, 248 kHz sonar described in I. Reflection from clouds of bubbles can be seen below the surface extending down to 6 m. Figure 2 shows a sonograph, range versus time, from a dual-beam side-scan sonar at the same location in similar wind conditions (see Thorpe & Hall 1983). The bands being advected by tidal currents across the display are due to the intense reflection of sound from lines of subsurface bubble clouds. These lines are orientated in the direction of the wind and are visible only when the wind exceeds about 7 m s^{-2} (or in lighter winds during heavy rainfall). The mean separation between bands is consistent with that observed between wind rows, and it is thus plausible that they result from Langmuir circulation and hence that this has an important effect on the instantaneous distribution of subsurface bubbles. This contention is supported by a calculation (see Appendix A) of the depth to which bubbles may be carried by the downward velocities observed beneath wind rows. The predicted depths compare favourably with the observed maximum bubble depths.

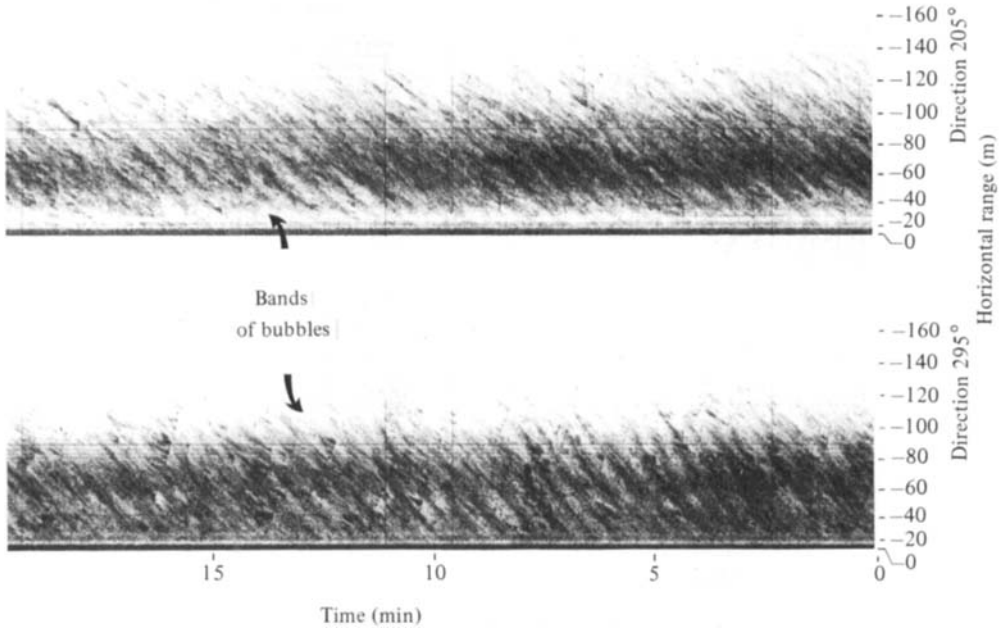

FIGURE 2. Sonographs, horizontal-range-versus-time displays, of bubble clouds obtained by a dual-beam side-scan sonar. The wind was about 8 m s^{-1}. (From Thorpe & Hall (1983).)

Further evidence of the effect of Langmuir circulation on subsurface particles may be found in the studies of the sinking of SARGASSUM (Johnson & Richardson 1977) or of the distribution of zooplankton (George & Edwards 1973).

In Appendix B we estimate the vertical flux of heat produced by Langmuir circulation based on the observations of vertical velocities by Filatov *et al.* (1981) and the temperature distributions of Thorpe & Hall (1982). The effective vertical diffusion coefficients K_v are found to be about 0.2–0.4 of those estimated to include all effects at comparable wind speeds (figure 11). The possible errors in estimates are, however, considerable, and the conclusion is perhaps most fairly stated as a finding that the contribution to K_v from Langmuir circulation alone is a significant fraction of the net value.

In view of these results and the possibility of making further acoustic studies, it appears worthwhile to model the effects that Langmuir circulation may have on submerged bubbles. There are also other reasons for doing this. Photographic observations of bubbles have been made by Johnson & Cooke (1979) using a freely drifting camera supported by a surface float. Since the float will tend to be carried by Langmuir circulation into wind rows, the bubbles sampled may not be typical of those found generally near the sea surface. Models of subsurface bubbles (I and Thorpe 1984*a*) find that the position of the peak in the distribution of bubble sizes tends to smaller radii as depth increases. Johnson & Cooke observed no such trend. Could the difference be due to biased sampling, primarily from regions of convergence below wind rows? The effect of Langmuir circulation on estimates of K_v using sonar (Thorpe 1984*b*) also deserves attention, and is examined in Appendix C.

In §2 we discuss an analytical model in which Langmuir circulation is represented as a perturbation on a primarily diffusive solution. This enables us to examine the effects of the circulation, and the model is later used to test a random-walk numerical simulation of turbulence which, once validated, is employed to describe details of bubble distributions in Langmuir circulation.

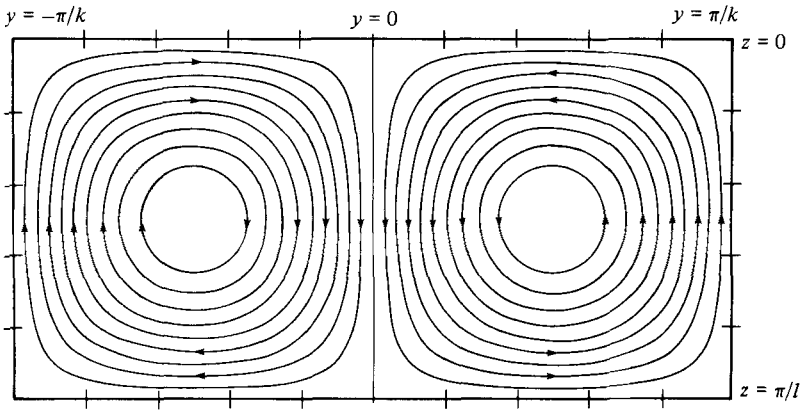

FIGURE 3. The circulation pattern imposed in the analytical solutions and numerical experiments.

2. An analytical model

2.1. *The model equation and its solution*

The simplest model including the effects of bubble diffusion by turbulence, the rise of bubbles, the dissolving of their gas into the surrounding water, and a flow resembling Langmuir circulation, is embodied in the equation

$$v\frac{\partial N}{\partial y}+(w-w_{\mathrm{b}})\frac{\partial N}{\partial z}=K_{\mathrm{h}}\frac{\partial^2 N}{\partial y^2}+K_{\mathrm{v}}\frac{\partial^2 N}{\partial z^2}-\sigma N, \tag{1}$$

with boundary condition

$$N\to 0 \quad \text{as} \quad z\to\infty, \tag{2}$$

where (y, z) are the horizontal and (downward) vertical coordinates, $z = 0$ representing the surface where bubbles are produced; $(v, w) = \epsilon(\partial\psi/\partial z, -\partial\psi/\partial y)$, and ψ is the stream function, $\psi = -Wk^{-1}\sin ky \sin lz$, of a repeated cell pattern with maximum vertical speed W and cell dimensions πk^{-1} and πl^{-1}. The circulation pattern in $-\pi k^{-1} \leqslant y \leqslant \pi k^{-1}$, $0 \leqslant z \leqslant \pi l^{-1}$ is shown in figure 3. The wind-row spacing is $2\pi k^{-1}$. Here ϵ is an ordering parameter put equal to unity in calculations, w_{b} is the speed at which bubbles rise through quiescent fluid, and K_{h}, K_{v} are horizontal and vertical diffusion coefficients, supposed constant. σ is an inverse timescale describing a decay due to the rate of loss of gas and N is the number of bubbles per unit volume at (y, z).

The formulation of (1) with $\psi = 0$, $K_{\mathrm{h}} = 0$, is discussed in I (§4.3.1) and solutions are given there and in Thorpe (1984*b*). Equation (1) may be regarded as a steady-state description of the concentration of bubbles of a given radius a_0, which are lost at rate σ (a crude representation of dissolution), and which rise at a constant rate w_{b}. In the numerical examples and when examining the importance of different terms we shall take $a_0 = 50$ μm, with corresponding $w_{\mathrm{b}} = 0.54$ cm s^{-1}, since this represents the radius of the peak in the bubble size distribution found by Johnson & Cooke (1979). A value of $\sigma = 0.018$ s^{-1} is consistent with observations of bubble lifetimes by Thorpe & Hall (1983) and with model results (Thorpe 1984*b*). The chosen form of ψ fails to reproduce some features of Langmuir circulation, for example the displacement of the centre of the circulation towards the position of the wind row, but nevertheless contains the main features. The indefinite repetition of the circulation pattern in the

vertical is unimportant provided that N is sufficiently small at $z = \pi l^{-1}$, the bottom of the uppermost cell.

When $W = 0$, (1) has solution $N \propto \exp(-\alpha z)$, where

$$\alpha = \frac{1}{2K_v}[w_b + N(w_b^2 + 4K_v\sigma)^{\frac{1}{2}}]. \tag{3}$$

Two seperate limits may be considered,

$$w_b^2/4\sigma K_v \gg 1, \tag{4}$$

when $\alpha \approx w_b/K_v$ and dissolution of gas from the bubbles is negligible in the diffusion equation, and

$$w_b^2/4\sigma K_v \ll 1, \tag{5}$$

when $\alpha \approx (\sigma/K_v)^{\frac{1}{2}}$ and bubble rise is negligible. (If $K_v = 0$ there is no mechanism to carry bubbles downwards from the surface, and their concentration N must be zero for $z > 0$ for all σ and $w_b > 0$.) Since, for the selected values, $w_b^2/4\sigma = 4.05$ cm^2 s^{-1}, (5) is likely to apply in most conditions (see figure 11 for estimates of K_v).

When $K_v = K_h = 0$ and $\sigma = 0$, the equation reduces to that discussed by Stommel (1952), who found that the particle (bubble) orbits may be closed when $\epsilon W > w_b$, allowing trapping even though $w_b > 0$. Since we here have $w = 0$ at $z = 0$ (the source of the bubbles) and the region of closed circulation is totally subsurface, there is no mechanism whereby bubbles can be carried into the closed regions. A finite value of K_v is essential. When, however, K_v and K_h are non-zero the regions of closed circulation can lose particles by diffusion and permanent trapping is no longer possible. Trapping may nevertheless lead to enhanced concentrations (Leibovich & Lumley 1982). The closed streamlines defined by Stommel reach a minimum depth

$$z_0 = \frac{1}{l}\sin^{-1}\frac{w_b}{\epsilon W} \tag{6}$$

at $y = 0$. If α^{-1}(defined in (3)) $\ll z_0$ few bubbles will enter the region of closed circulation whilst if $\alpha^{-1} \gg z_0$ the region of closed circulation will be efficiently fed by bubbles from the surface and the effect of Langmuir circulation on the downward transport may be considerable. When, as in (5), $\alpha \approx (\sigma/K_v)^{\frac{1}{2}}$ the condition that Langmuir circulation should be important becomes

$$\epsilon W \gg \frac{w_b}{\sin(l(K_v/\sigma)^{\frac{1}{2}})}, \quad \equiv W_c \text{ say}. \tag{7}$$

If, for example, $K_v = 180$ cm^2 s^{-1} and the cell depth is 5 m, $l = 2\pi/10$ rad m^{-1} and we find $W_c = 0.92$ cm s^{-1} for $\sigma = 0.018$ s^{-1}. This compares with values of ϵW observed by Filatov *et al.* of 1–4 cm s^{-1}. An additional condition for the circulation to produce significantly enhanced concentrations of bubbles is that bubbles produced by waves breaking between the wind rows may be carried horizontally for an appreciable part of the width of the cell in time σ^{-1} before they decay. Bubbles near the surface are carried from $y = \frac{1}{2}\pi k^{-1}$ to $\frac{1}{4}\pi k^{-1}$ in a time $(\epsilon W l)^{-1}\log(1/\tan\frac{1}{8}\pi)$, hence for the circulation to redistribute the bubbles significantly we need

$$\epsilon W \gtrsim 0.38\sigma l^{-1}, \quad = 1.1 \text{ cm s}^{-1} \tag{8}$$

for the values of σ and l used above.

The necessity to have a non-zero K_v to provide a mechanism to feed bubbles into the region in which Langmuir circulation may be effective suggested that it would

be profitable to examine a perturbation about an initial state defined by $W = 0$, rather than the special case in which $K_v = 0$ (when $N = 0$ for $z > 0$). This procedure will enable us to examine the basic effects of Langmuir circulation on a primarily diffusive solution.

We therefore solve (1), seeking a solution in which N is expressed as a power series in ϵ:

$$N = N_0(y,z) + \epsilon N_1(y,z) + \epsilon^2 N_2(y,z) + \dots . \tag{9}$$

Successive terms are determined by comparing coefficients of ascending orders of ϵ when (9) is substituted into (1), subject to (2) and an appropriate boundary condition at $z = 0$. We consider two possible candidates for the latter, either

$$N = n, \quad \text{a constant}, \tag{10}$$

giving a uniform concentration of bubbles at the surface, or

$$K_V \frac{\partial N}{\partial z} = -F, \quad \text{a constant}, \tag{11}$$

representing uniform downward diffusive flux into the ocean over the ocean surface. The latter condition appears most realistic, corresponding to a statistically uniform production of bubbles by raindrops, spray or randomly breaking waves. (No correlation between the position of wave breaking and wind rows was found by Kenney (1977) or by Thorpe & Hall (1980), and thus an assumption of uniformity appears valid.)

We shall find it useful to write down the results in terms of parameters

$$\theta = \frac{W}{2lK_v}, \quad \phi = \frac{w_b}{2lK_v}, \quad q = \frac{1}{l}\left(\frac{\sigma}{K_v}\right)^{\frac{1}{2}}, \quad \zeta = \frac{k^2 K_h}{l^2 K_v}. \tag{12}$$

Here θ is a measure of the effect of the circulation, and ϕ is a measure of the importance of bubble rise. Equation (5) implies that $\phi^2 \gg q^2$. A necessary condition for ignoring the effect of the vertical repetition of the circulation cells in the model, is that α^{-1} is much less than πl^{-1}, or that

$$q_1 = \alpha l^{-1} \gg 1. \tag{13}$$

Since

$$q_1 = \phi + (\phi^2 + q^2)^{\frac{1}{2}} \tag{14}$$

the condition (13) is satisfied if q is sufficiently large. The effects of cell geometry and K_h different from K_v are incorporated in ζ.

The solution is, at order ϵ^0,

$$N_0 = n_0 e^{-\alpha z}, \tag{15}$$

where $n_0 = n$ (boundary condition (10)) or $n_0 = F/\alpha K_v$ (boundary condition (11)), which is independent of y and hence of K_h.

At order ϵ^1

$$N_1 = n_0 \cos ky\,[e^{-\alpha y}(A \sin lz + B \cos lz) + C e^{-\beta z}], \tag{16}$$

where

$$A = \frac{2\theta q_1(1+\zeta)}{(1+\zeta)^2 + 4(\phi^2+q^2)}, \quad B = \frac{-4\theta q_1(\phi^2+q^2)^{\frac{1}{2}}}{(1+\zeta)^2 + 4(\phi^2+q^2)} \quad \beta = l[\phi + (\phi^2+q^2+\zeta)^{\frac{1}{2}}]$$

and

$$C = \begin{cases} -B & \text{(boundary condition (10))} \\ \dfrac{lA - \alpha B}{\beta} & \text{(boundary condition (11)).} \end{cases}$$

The y-averaged value of N_1 is zero, and hence the mean vertical profile is unchanged.

At order ϵ^2 a solution is found of the form

$$N_2 = n_0\{e^{-\alpha z}[r+az+b\sin 2lz+c\cos 2lz + \cos 2ky(d+f\sin 2lz+g\cos 2lz)]+e^{-\beta z}[j\sin lz+h\cos lz + \cos 2ky(p\sin lz+m\cos lz)]+te^{-\gamma z}\cos 2ky\}, \quad (17)$$

where

$$\gamma = l[\phi+(\phi^2+q^2+4\zeta)^{\frac{1}{2}}].$$

The y-averaged value of N_2 is, in general, non-zero, so that the mean vertical profile is no longer that of the exponential form of (15). The effect of large horizontal diffusivity (large ζ) is to reduce the size of the coefficients in N_1 and N_2.

The coefficients in (17) and the solution for N_3 for $\zeta = 1$ and $\phi = 0$, together with $\overline{N}_4$, the y-averaged value of N_4, have been calculated. (Details are available on request from the Editor or author.) The coefficients of terms in ϵ^m are of order θ^m, and for some sufficiently small $\epsilon\theta$ (a function of ϕ, q and ζ) we may expect that (9) will be convergent and that the leading terms will give a satisfactory approximation to the bubble concentration N.

The effect of the circulation on the concentration is illustrated in figure 4, showing contours of constant $\log_{10} N$ for $\phi = 0$ (no bubble rise), $l = k$, $K_v = K_h$, $q = 3$ with boundary condition (10) and for various θ. The effect of the circulation is to increase the concentration in the vicinity of downgoing fluid (see figure 3). The second and higher harmonics produce an asymmetry in lines of uniform concentration, the width of the downward-pointing 'peak' near the surface being relatively narrow, a feature reminiscent of the pattern of high-temperature anomaly below wind rows (Thorpe & Hall 1982). At $\theta = 3.0$ the concentration distribution in the upward-going parts of the circulation has an undular structure, suggesting that the convergence is no longer satisfactory, although this occurs only at relatively small concentrations.

2.2. *The vertical flux*

The solution can be used to find the vertical flux associated with the circulation. The total vertical flux produced by diffusion and advection is

$$F_v = \overline{wN} - K_v\frac{\overline{\partial N}}{\partial z},$$

where the bar represents averages over y. We may write F_v in terms of an effective vertical diffusion coefficient K_{ve}:

$$F_v = -K_{ve}\frac{\overline{\partial N}}{\partial z},$$

so that

$$\frac{K_{ve}-K_v}{K_v} = -\frac{\overline{wN}}{K_v\,\overline{\partial N/\partial z}}.$$

This may easily be found, correct to second order, by substituting for N from (9), using (15)–(17) and $w = W\cos ky\sin lz$. Unlike K_v, which depends only on the turbulent motion, K_{ve} depends on the values of ϕ and q as well as on θ and ζ, and is thus a function of the properties of the bubbles as well as of the scales of the imposed motions. It is thus not possible to define unambiguously an effective diffusion coefficient dependent only on the turbulence and motion in the water. For some particular values of the parameters, K_{ve}/K_v is shown in figure 5 as a function of z. The accuracy of the determination of K_{ve} from acoustic measurements is discussed

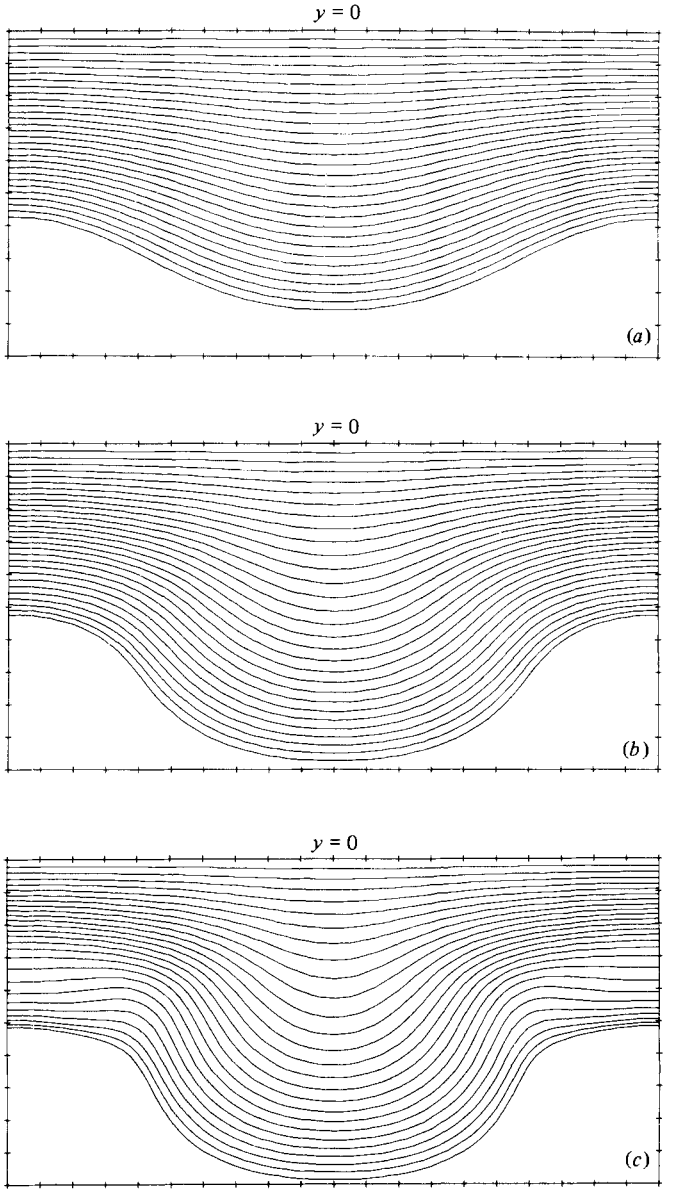

FIGURE 4. Contours of $\log_{10} N$ at 0.1 intervals estimated to third order in ϵ for $\phi = 0$, $q = 3$, $\zeta = 1$, and at (*a*) $\theta = 1$; (*b*) 2; (*c*) 3, using boundary condition (10).

in Appendix C. It appears that the effective diffusion coefficient (and hence the flux) may generally be found to better than 25 %.

The analytical solution, however, appears valid only for sufficiently small values of $\epsilon\theta$ – smaller than those generally observed. Its value lies in providing illustration of the effects of weak circulation on the near-surface distribution of bubbles and in establishing the validity of the numerical model which we now describe.

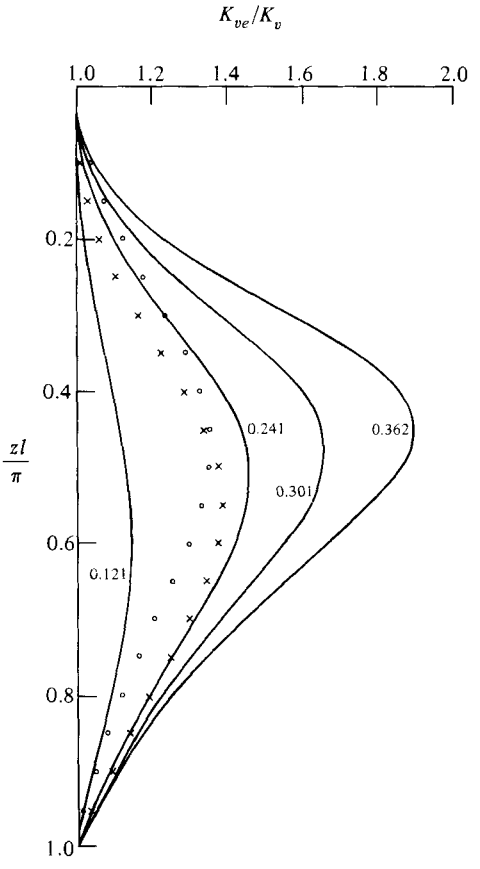

FIGURE 5. K_{ve}/K_v plotted as a function of depth z from the analytical solution with boundary condition (11) at $\phi = 0.651$, $q = 2.63$. The lines are for $\zeta = 1$ at various marked values of θ. The crosses are for $\theta = 1.205$, $\zeta = 0.1$ and circles are $\theta = 1.205$, $\zeta = 10$.

3. A numerical model

In Thorpe (1984*a*) we described a numerical model of the motion of subsurface bubbles. Turbulence is simulated by displacements of the water surrounding a bubble through a distance L in a random direction δ in (y, z)-space at each time step ΔT. Superimposing the vertical motion of the bubble w_b and mean currents $v(y, z)$, $w(y, z)$ as defined in (1), the bubble displacements are

$$\Delta y = v\,\Delta T + L\sin\delta,$$

$$\Delta z = (w - w_b)\,\Delta T + L\cos\delta,$$

where w_b is now a function of bubble radius. At each time step the radius of the bubble a is changed according to a first-order finite-difference representation of an equation representing the change in bubble radius

$$\frac{da}{dt} = \dot{a}_1 + \dot{a}_2,$$

where $\dot{a}_1$ is a rate of change due to gas flux from the bubbles into the surrounding water, and $\dot{a}_2$ is the change due to pressure variation. The bubbles are supposed to

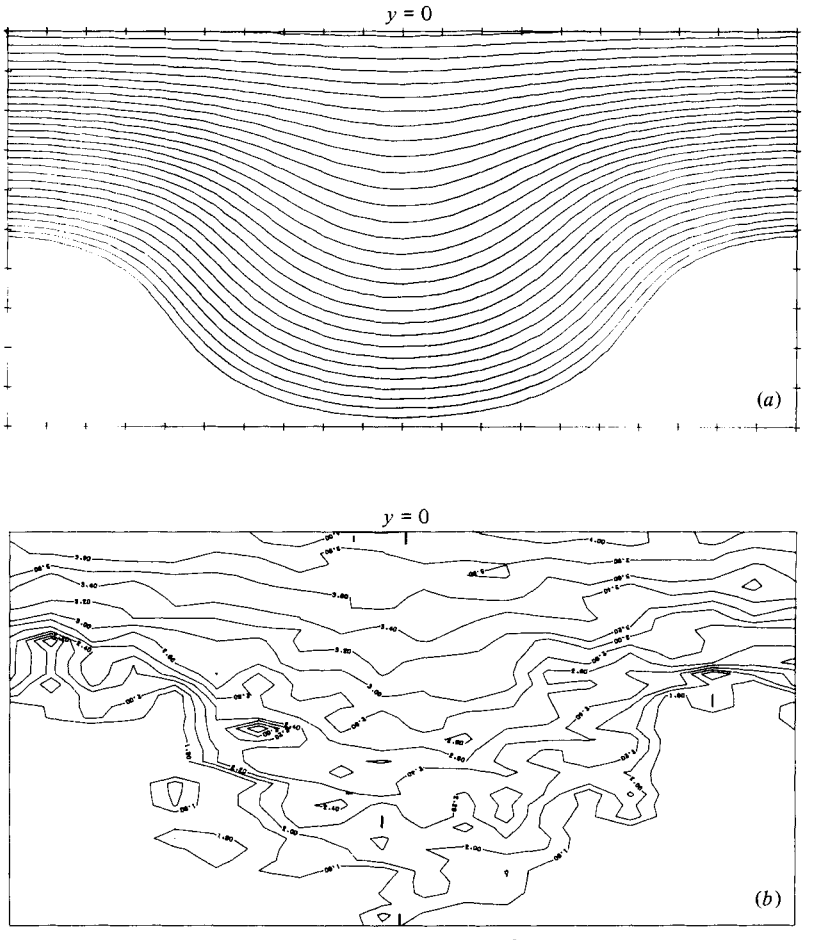

FIGURE 6(*a*, *b*). For caption see facing page.

be composed of two gases with parameters selected for oxygen and nitrogen; x is the mole fraction of oxygen. This also changes in time according to a finite-difference equation. Expressions for $\dot{a}_1$, $\dot{a}_2$ and x, and the equations adopted for w_b and the Nusselt numbers, and values of parameters adopted in the numerical calculations, are given in I. Bubbles with a range of different sizes are introduced at random positions in $-\pi k^{-1} < y < \pi k^{-1}$ at each time step, and their positions, radii, and gas fractions are followed. Those subsequently reaching $z = 0$ or having $a < 1$ μm are discarded. Those crossing the vertical boundaries at $y = \pm\pi k^{-1}$ are reintroduced at the opposite boundary. The model is run until a steady state is reached, typically after about 7 r^{-1}, i.e. 400 s.

The turbulent-diffusion coefficient $K_v = K_h$ is given by

$$K_v = L^2/4\Delta T$$

(Csanady 1973). The model was first run with $v = w = 0$ and with bubbles having $w_b = 0.54$ cm s^{-1} and decaying at rate $\sigma = 0.018$ s^{-1}, as in §2. Equation (3), with $\theta = 0$, was used to test the value of K_v. The solutions were then compared with the analytical solutions in §2 in conditions when θ was sufficiently small for good convergence. As an example, figures 6(*a*, *b*) show comparative contours of $\log_{10} N$ for

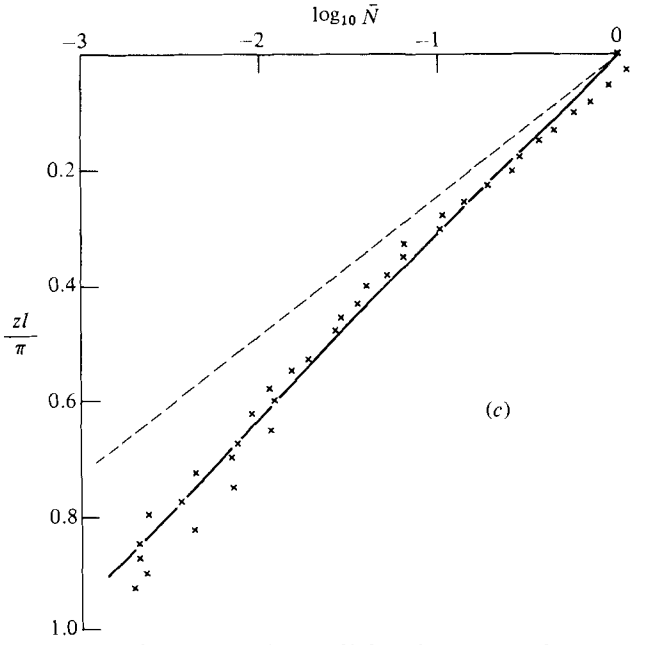

FIGURE 6. (*a*, *b*) Comparison of contours of $\log_{10} N$ found by (*a*) analytical solution (§2) and (*b*) numerical solution (§3) for $\theta = 2$, $\phi = 0$, $q = 3$, $l = k$, $K_h = K_v$. The contours are at intervals of (*a*) 0.1, (*b*) 0.2. (*c*) $\log_{10} \bar{N}$ versus depth for analytical solution (solid lines) and numerical solution (points). $\bar{N}$ is normalized to unity at $z = 0$. The dashed line is the analytical solution (3) for $\theta = 0$ (no circulation).

$\theta = 2.0$, $\phi = 0$, $q = 3$, $l = k$, whilst figure 6(*c*) shows the vertical mean profiles. The agreement appeared to be generally satisfactory. An increase in $\bar{N}$ at depth is the principal effect of Langmuir circulation on the mean profile.

Further runs were made using the full description of bubbles, including radius variation, with 600 bubbles of each size $10m$ μm, $1 \leqslant m \leqslant 20$, being introduced at each time step of length 5 s. A steady state was judged to have been reached after 400 s. The cell width and depths were made to be equal to 5 m corresponding to a distance between wind rows of 10 m, which is fairly typical. One objective was to compare our results with those described in Thorpe (1984*a*) where, to relate results to those of Johnson & Cooke (1979), we focused attention on $K_v = 180$ cm^2 s^{-1} and assumed that water was just saturated with oxygen and nitrogen so that, at the surface, $x = 0.215$ corresponds to an air mixture of the gases. We have adopted these values here. In order to reproduce a distribution of bubbles which resembles those observed, we have introduced bias factors; the numbers of bubbles of each size introduced at the surface are scaled to produce a distribution at 0.7 m which is a smoothed version of that observed by Johnson & Cooke (1979).

Figure 7 shows the horizontally averaged distributions of bubble sizes at 1.8 m and 4.0 m. The stepped distributions are smoothed versions of those observed by Johnson & Cooke drawn for 10 μm radius bins. The effect of increasing θ is to enhance the number of bubbles found at depth, but to produce little change in the position of the peak in the model distribution which, as found in other models (see I), tends to smaller radii as depth increases. A similar trend was found when only the bubbles in $-\frac{1}{6}\pi k^{-1} < y < \frac{1}{6}\pi k^{-1}$ were used, to simulate conditions in which sampling was predominantly in the regions of convergence near wind rows. It thus appears unlikely

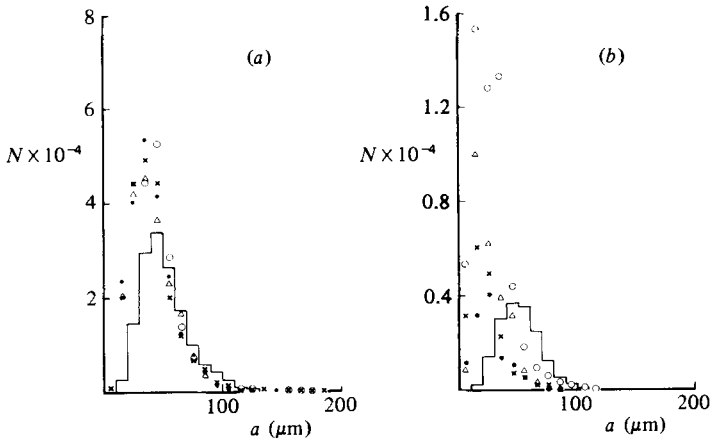

FIGURE 7. The horizontally averaged distribution of bubbles at (*a*) 1.8 m and (*b*) 4.0 m. N is the number of bubbles/m^3 per 10 μm radius band. The stepped histograms are interpolated from data obtained by Johnson & Cooke (1979) in winds of 11–13 m s^{-1}. The points are model results at ●, $\theta = 0$; ×, 0.44; △, 0.88; ○, 1.77, in which the distributions have been fitted to the observations at 0.7 m.

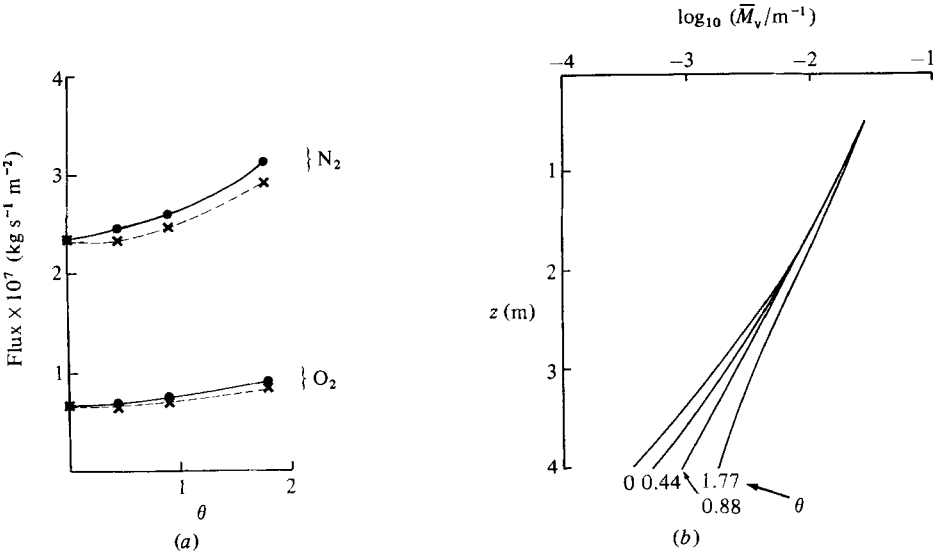

FIGURE 8. (*a*) The gas flux of nitrogen and oxygen from the bubbles into the water as a function of θ. The full curve is from bubble distributions which are matched to that observed by Johnson & Cooke (1979) at 0.7 m. The dashed curves are fluxes estimated by assuming that the input of bubbles at the surface remains unchanged as θ increases, and equal to that which matches Johnson & Cooke's observed distribution at $\theta = 0$. (*b*) The horizontally averaged acoustic scattering cross-section of the bubbles per unit volume $\overline{M}_v$ plotted on a log scale versus depth z at different values of θ. The surface input of bubbles is that corresponding to the dashed curves in (*a*) and is thus independent of θ.

that the failure to describe the observed peak at 50 μm correctly is due to the omission of an explicit representation of Langmuir circulation in earlier models, or that the position of the observed peak is an artifact of biased sampling, and we must look elsewhere for an explanation (for further discussion see Thorpe 1984*a*).

Figure 8 (*a*) shows the effect of θ in increasing the flux of the gases from the bubbles

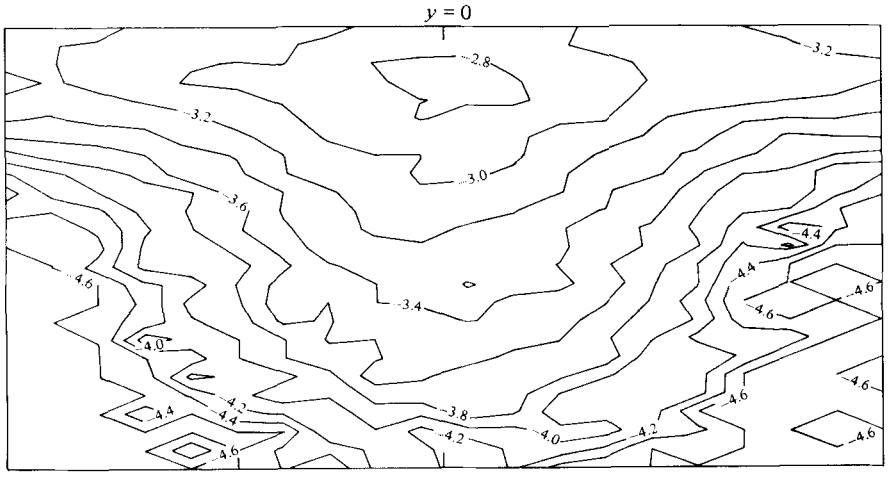

FIGURE 9. Contours of $\log_{10} M_v$ in intervals of 0.2 at $\theta = 1.77$. The conditions were the same as in figure 8(*b*).

into the water. The flux is found by summing the flux from individual bubbles when the steady state is reached. This flux does not include the direct exchange of gases between the air and the water across the water surface (see Thorpe 1984*c*). Figure 8(*b*) shows vertical profiles of $\log_{10} \overline{M}_v$, where M_v is the acoustic scattering cross-section of the bubbles per unit volume and the overbar denotes a horizontal average. The presence of the circulation increases $\overline{M}_v$ at depth. Figure 9 is a contour plot of $\log_{10} M_v$ at $\theta = 1.77$. This represents a circulation speed W of 4 cm s^{-1}, which is that observed by Filatov *et al.* (1981) in winds of about 12 m s^{-1} in which Johnson & Cooke made their measurements. It is interesting to note the highly scattering core of bubbles below the surface at the centre of the convergent region at $y = 0$, where partial trapping by the Stommel mechanism is effective. The enhanced scattering here is of sufficient magnitude to be easily detected by sonar and is in accordance with the observations presented in figures 1 and 2 and the measurements of M_v in I.

4. Discussion

The comparison of the bubble-cloud depths predicted using the measurements of vertical velocities below wind rows by Filatov *et al.* (1981) and the maximum depths observed (Appendix A), and the estimates of heat flux by Langmuir circulation (Appendix B), provide circumstantial evidence for the importance and significance of Langmuir circulation in the near-surface mixing layer. The calculations in §§2 and 3 demonstrate that Langmuir circulation should produce a distortion in the distribution of subsurface bubbles (e.g. figures 6 and 9), which, provided their input at the surface is fairly uniform (as in heavy rain) or frequent (as in strong winds), should easily be detected by side-scan sonar, as is indeed the case (Thorpe & Hall 1983).

The central difficulty is the appropriate representation of turbulence. We have here, for simplicity, assumed that it can be described by a diffusion coefficient which is independent of depth and of the imposed circulation, as though turbulence could be regarded as a uniform diffusive process acting on a mean circulation, but we are left with the problem of how to select appropriate values for K_v. The values shown

in figure 11 are estimated from observations which do not distinguish between circulations and turbulence, and which embody the effects of all processes contributing to the vertical diffusion of bubbles. Perhaps it is not unreasonable to include Langmuir circulation within the representation of turbulence? The distance between neighbouring wind rows has a broadband structure (see McLeish 1968, figure 4; Thorpe & Hall 1982, figure 2; Ryanzhin 1982), and we have detected no significant peaks in the horizontal, cross-wind, temperature spectra at scales corresponding to the wind rows at depth of 1–4 m. The wind rows are transient. Observations at fixed position suggest lifetimes of 5–20 min, although Kenney (1977) reports rows persisting for an hour in a shallow area of the Lake of the Woods in Canada. If, however, the theoretical studies of Craik and Leibovich are correct in relating the circulation to the interaction between surface waves and the currents (Leibovich 1983), then to regard them simply as large coherent eddies in a turbulent field is to denigrate their specific role in transferring energy from the wave field, and neglects a possibly fruitful method of approaching turbulent diffusion by imposing a separation of scales which, as here, allows examination of interacting processes.

The enhancement of the vertical flux by circulation, which was discussed in §2.2, suggests that the value of K_v adopted in §3 from figure 11 for comparison with Johnson & Cooke's observations in winds of 11–12 m s^{-1} was too large when Langmuir circulation is included in the model. The results may underestimate the importance of the circulation; the value of θ used in figure 9 is perhaps too small. Our objective was, however, to examine the primary effects of the circulation on a diffusive process and to gauge their magnitude. An important conclusion is that the values of M_v at depth are greatly enhanced by the circulation (see figure 8*b*). In I we found that the observed value of the lengthscale

$$d = \left(-\frac{1}{M_v} \frac{\mathrm{d}M_v}{\mathrm{d}z} \right)^{-1}$$

in winds exceeding 10 m s^{-1} was too large to be explained by the use of a diffusion coefficient $K_v = ku_* z$, where u_* is the friction velocity in the water, and k is von Kármán's constant, appropriate in the atmospheric boundary layer over land in conditions of neutral stability. In Thorpe (1984*b*) we considered whether turbulence induced by surface waves might contribute to the discrepancy. This was likely only if the depth of influence of wave-induced turbulence extends to some fourteen times the r.m.s. wave amplitude. The present results suggest that the increase in d may be more plausibly explained by the presence of Langmuir circulation.

Dr Mel Briscoe invited me to give a 'tutorial' paper on Langmuir Circulation at the 1982 Fall Meeting of the AGU and rekindled my interest. I am grateful to Professor S. Leibovich for allowing me to see a draft version of his 1983 review paper and for drawing my attention to his paper with Professor Lumley.

Appendix A. Maximum depth of bubble clouds

In I we estimated the maximum depth to which bubbles composed of an air mixture of oxygen and nitrogen could be carried from the surface by a steady and uniform vertical downward velocity. Included in the calculation were the effects of the bubbles' buoyant rise (a function of bubble radius) opposing the downward velocity, the compression of bubbles as depth increased, and the loss of gas to the surrounding water by dissolution. There is evidence that bubbles produced naturally in the sea

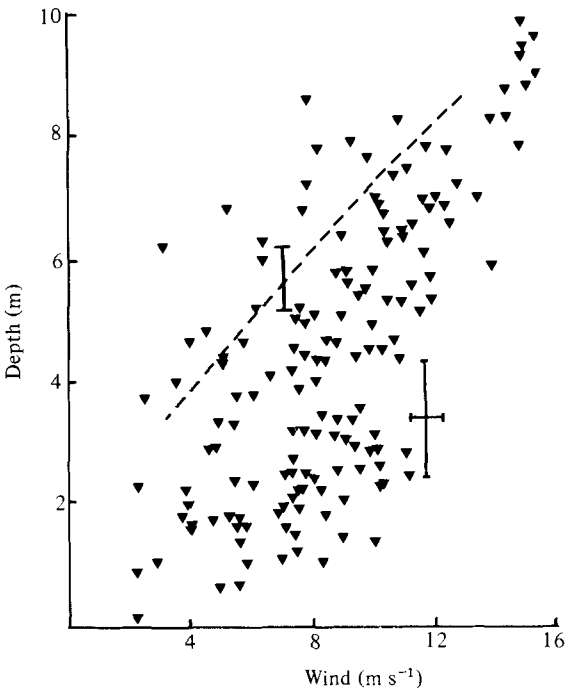

FIGURE 10. The maximum depth of bubble clouds *vs.* mean wind speed estimated at 10 m above the water surface. The points are the maximum depths observed in 1 h periods in the sea near Oban (see I). The dashed line is the estimated depth derived from vertical velocities below wind rows. The cross shows the estimated errors in both points and the dashed line, and the vertical bar indicates the change in position of the dashed line brought about by varying the saturation level of the gases in the water by $\pm 4\%$.

rapidly become covered by a surface-active film which renders their surface immobile; and this is accounted for in the calculation.

The flow pattern used in the calculation in I is unrealistic since the mean vertical velocity at the surface is non-zero, but nevertheless it provides an estimate which reflects, in its approximate nature, the lack of information about the structure of the vertical currents below wind rows. We have therefore combined the depth estimates (see I, figure 20*a*) with the vertical velocities measured below wind rows by Filatov *et al.* (1981), at various wind speeds, to predict the maximum depth to which 'dirty' bubbles will be carried before they dissolve in water saturated in oxygen and nitrogen. This is shown as a function of wind speed by the dashed line in figure 10 together with the maximum depths averaged over 1 h periods of bubble clouds observed using sonar near Oban (from I, figure 15*b*). The latter show considerable scatter. This might be expected, since bubble clouds are patchy, bubbles being supplied in a random way when and where waves break, and wind rows, if present, will rarely be directly over the sonar used to measure the bubble-cloud depth. The maximum observed depth is of course related to the minimum detection level of the bubbles. The curve does however provide a reasonable upper bound within the estimated errors of observation. The estimates of vertical velocities by Harris & Lott (1973) were approximately twice those found by Filatov *et al.* at comparable wind speeds; were of smaller magnitude when the stability of the near-surface water was negative, contrary to the observations of Filatov *et al.* and to the observations in I of an increase in bubble depth when the

air–water temperature difference was negative; and would lead to an estimate of the maximum bubble depth well in excess of that observed. We are thus led to conclude that the observations by Filatov *et al.* of vertical speeds below wind rows are consistent with our observations of bubble clouds, and that Langmuir circulation will influence cloud depth and induces vertical velocities which are comparable in magnitude to the largest produced and sustained over the lifetime of bubbles (a few minutes; Thorpe & Hall 1983) in the mixing layer.

It is assumed in making these estimates that the circulation extends to at least the depth of the deepest observed bubble clouds. Our early observations (Thorpe & Stubbs 1979) showed that bubbles were not seen to extend down as far as the top of the stable thermocline. A conclusion of that work, the finding that no clear correlation could be found between cloud depth and the presence of wind rows, was later qualified (Thorpe & Hall 1982) by more careful observations in which a statistically significant correlation was found between the acoustic scattering cross-section per unit volume of the bubble clouds M_v at small depths (< 2.3 m) and the presence of wind rows. This, and the side-scan observations shown in figure 2, suggest that the earlier conclusion was incorrect and that a correlation between wind rows and cloud depth may be found if care is taken to obtain statistically robust data. The correlation, though significant, is probably weak and barely detectable from other natural variations, as is that of the correlation of temperature with wind rows (Thorpe & Hall 1982). The large scatter of points in figure 10 bears out this conclusion.

Appendix B. Estimates of vertical flux

We may estimate the vertical flux produced by Langmuir circulation by combining the observations of Filatov *et al.* (1981) with those of Thorpe & Hall (1982). The latter measured the mean temperature gradient $\mathrm{d}T/\mathrm{d}z$ in Loch Ness† and the mean temperature anomalies t in the water below wind rows on three different occasions, sampling extending over more than 100 wind rows in each. The vertical flux $\overline{w't'}$, averaged over the width of a wind row, may be estimated as $\frac{1}{2}wt$. Here w' is the vertical velocity, t' is temperature and w is the vertical velocity below a wind row, which may be estimated from the data of Filatov *et al.* at wind speeds corresponding to those of Thorpe & Hall's observations. A vertical diffusion coefficient K_v representing the advective flux is given by

$$K_v \frac{\mathrm{d}T}{\mathrm{d}z} = \overline{w't'} \approx -\tfrac{1}{2}wt,$$

and K_v may thus be found. The values are shown as functions of the wind speed W_{10} by the squares in figure 11.

Also shown for comparison in figure 11 are values of the net vertical diffusivity, assumed independent of depth and determined from acoustic measurements of the bubbles as described by Thorpe (1984*b*). These are significantly higher than the previous estimates based on the flux of heat by Langmuir circulation. It is not established that the eddy-diffusion coefficients for heat and bubble transport should be the same, but since those of heat and momentum are almost equal in conditions

† The maximum depths of bubble clouds in Loch Ness were not observed as often or over as wide a range of wind speeds as were those at Oban (see I, figure 10*b*), but were reasonably consistent with them, and we are thus justified here in using the data of Filatov *et al.* on vertical velocities (see Appendix A).

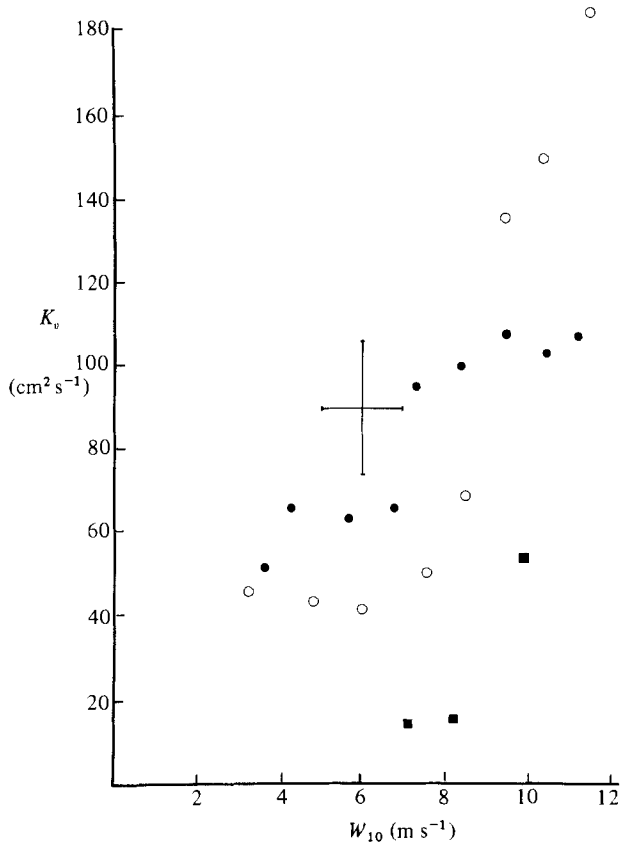

FIGURE 11. The variation of vertical diffusion coefficient K_v with wind speed: ■, from the temperature anomaly and vertical velocities below wind rows; ●, from observations of bubbles in Loch Ness; ○, from observations of bubbles in the sea near Oban (see Thorpe 1984*b*).

of high Reynolds number and low Richardson number (see e.g. Ueda, Mitsumoto & Komori 1981) like those found near to the sea surface, it might be expected that their values will not differ by very much. As expected the value of K_v estimated from the bubble profiles exceeds that found solely from advection in the Langmuir circulation pattern. It appears that 20–40 % of the net flux (perhaps more) may be carried by the circulation at wind speeds of 7–10 m s^{-1}. The possible errors are, however, considerable.

Appendix C. Estimation of K_{ve} by sonar

In Thorpe (1984*b*) we described how the value of the vertical turbulent diffusion coefficient might be determined from observations of the vertical distribution of the average acoustic scattering cross-section per unit volume $M_v(z)$ of subsurface bubbles. For bubbles of equal radii, M_v is proportional to N. In practice it is difficult to measure M_v accurately, but the slope

$$s = -\frac{1}{M_v}\frac{\mathrm{d}M_v}{\mathrm{d}z}$$

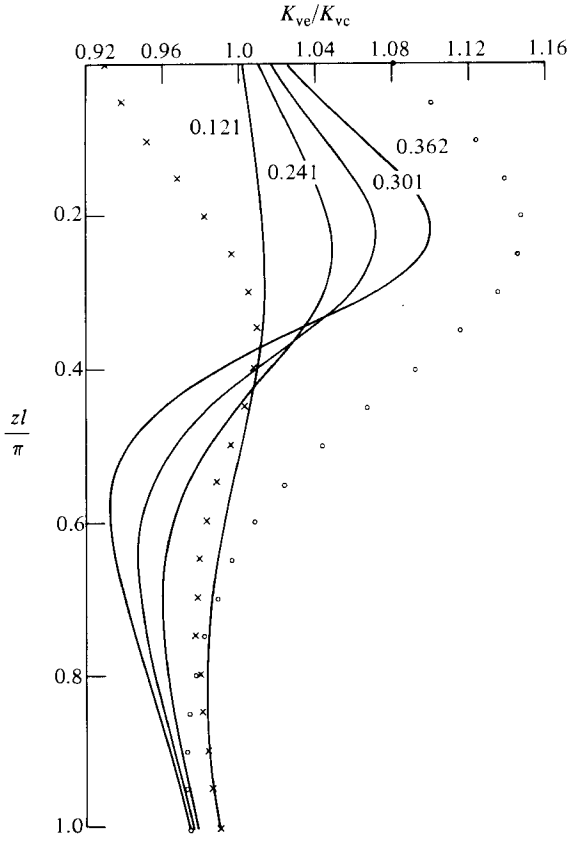

FIGURE 12. The ratio of the effective diffusion coefficient, K_{ve} to that estimated from the slope α, K_{vc}, as a function of depth at various marked values of θ at $\phi = 0.651$, $q = 2.63$. The lines are at $\zeta = 1$. The crosses are at $\theta = 1.205$, $\zeta = 0.1$, and the circles at $\theta = 1.205$ and $\zeta = 10$.

can be determined, at least locally. It is of interest to enquire how well K_{ve} might be determined from s, under the assumptions that there is no information about the circulation and that the best estimate will be found with a constant diffusion coefficient. Let this be K_{vc}, and assume that there is no circulation. Then, fitting the solution (3) to the measured s, we have

$$K_{vc} = w_b s^{-1} + \sigma s^{-2},$$

where

$$s = -\frac{1}{\bar{N}} \frac{d\bar{N}}{dz}.$$

This may be compared with the effective diffusivity K_{ve}. Figure 12 shows the ratio of the two diffusivities, plotted as functions of z, for the same values of parameters as were used in figure 5. The errors involved in using the slope to estimate the diffusion coefficient are, for the parameter range illustrated, less than 15%.

The ratio K_{ve}/K_{vc} is sensitive to ζ, or to the shape of the circulation cells, although the variation illustrated in figure 12 may be more than that which occurs naturally (see Leibovich 1983). The error in estimating the vertical diffusivity from the slope, measured by the parameter $|K_{ve}/K_{vc} - 1|$, increases as θ and ζ increase, and decreases as ϕ and q increase for $0 < \theta < 5$, $0.25 < \zeta < 4$, $0.1 < \phi < 1$ and $1 < q < 5$. The

parameter is less than 0.26 in this range of $\phi > 0.4$, $\phi < 2$, $q > 2$ and $\zeta \geqslant 1$. At $\zeta = 4$ and $q = 3$ the parameter is less than 0.25 if $\theta < 5$, $\phi > 0.1$.

REFERENCES

CSANADY, G. T. 1973 *Turbulent Diffusion in the Environment.* Reidel.

FALLER, A. J. & CAPONI, E. A. 1978 Laboratory studies of wind-driven Langmuir circulation. *J. Geophys. Res.* **83** (C7), 3617–3634.

FALLER, A. J. & CARTWRIGHT, R. W. 1982 Laboratory studies of Langmuir circulation. *Tech. Rep.* BN-985, *Inst. Phys. Sci. Tech., Univ. Maryland.*

FILATOV, N. N., RJANZHIN, S. V. & ZAYCEV, L. V. 1981 Investigation of turbulence and Langmuir circulation in Lake Ladoga. *J. Great Lakes Res.* **1**, 1–6.

GEORGE, D. G. & EDWARDS, R. W. 1973 Daphnia distribution within Langmuir circulations. *Limnol. Oceanogr.* **18**, 798–800.

HARRIS, G. P. & LOTT, J. N. A. 1973 Observations of Langmuir circulations in Lake Ontario. *Limnol. Oceanogr.* **18**, 584–589.

JOHNSON, B. D. & COOKE, R. C. 1979 Bubble populations and spectra in coastal waters: a photographic approach. *J. Geophys. Res.* **84** (C7), 3761–3766.

JOHNSON, D. L. & RICHARDSON, P. L. 1977 On the wind-induced sinking of Sargassum. *J. Exp. Mar. Biol. Ecol.* **28**, 255–267.

KENNEY, B. C. 1977 An experimental investigation of the fluctuating currents responsible for the generation of windrows. Ph.D. thesis, University of Waterloo, Ontario.

LANGMUIR, I. 1938 Surface water motion induced by wind. *Science* **87**, 119–123.

LEIBOVICH, S. 1983 The form and dynamics of Langmuir circulations. *Ann. Rev. Fluid Mech.* **15**, 391–427.

LEIBOVICH, S. & LUMLEY, J. L. 1982 Interaction of turbulence and Langmuir cells in vertical transport of oil droplets. In *Proc. 1st Intl Conf. on Meteorology and Air/Sea Interaction in the Coastal Zone, 10–14 May 1982, The Hague, Netherlands.*

MCLEISH, W. 1968 On the mechanism of wind-slick generation. *Deep-Sea Res.* **75**, 6872–6877.

POLLARD, R. T. 1977 Observations and theories of Langmuir circulations and their role in near surface mixing. In *A Voyage of Discovery: G. Deacon 70th Anniversary Volume* (ed. M. Angel), pp. 235–251. Pergamon.

RYANZHIN, S. V. 1982 On the cross sizes of Langmuir circulations' cells without the thermocline in lake. *Atmos. Oceanic Phys.* **18**, 1057–1065.

SCOTT, J. T., MYER, G. E., STEWART, R. & WALTHER, E. G. 1969 On the mechanism of Langmuir circulations and their role in epilimnion mixing. *Limnol. Oceanogr.* **14**, 493–503.

STOMMEL, H. 1949 Trajectories of small bodies sinking slowly through convection cells. *J. Mar. Res.* **8**, 24–29.

THORPE, S. A. 1982 On the clouds of bubbles formed by breaking wind waves in deep water, and their role in air–sea gas transfer. *Phil. Trans. R. Soc. Lond.* A **304**, 155–210.

THORPE, S. A. 1984*a* A model of the turbulent diffusion of bubbles below the sea surface. Submitted to *J. Phys. Oceanogr.*

THORPE, S. A. 1984*b* On the determination of K_v in the near-surface ocean from acoustic measurements of bubbles. *J. Phys. Oceanogr.* (to appear).

THORPE, S. A. 1984*c* The effect of bubbles produced by breaking wind-waves on gas flux across the sea surface. *Annales Geophys.* (to appear).

THORPE, S. A. & HALL, A. J. 1980 The mixing layer of Loch Ness. *J. Fluid Mech.* **101**, 687–703.

THORPE, S. A. & HALL, A. J. 1982 Observations of the thermal structure of Langmuir circulation. *J. Fluid Mech.* **114**, 237–250.

THORPE, S. A. & HALL, A. J. 1983 The characteristics of breaking waves, bubble clouds and near-surface currents observed using side-scan sonar. *Continental Shelf Res.* **1**, 353–384.

THORPE, S. A. & STUBBS, A. R. 1979 Bubbles in a freshwater lake. *Nature* **279**, 403–405.

UEDA, H., MITSUMOTO, S. & KOMORI, S. 1981 Buoyancy effects on the turbulent transport processes in the lower atmosphere. *Q. J. R. Met. Soc.* **107**, 561–578.